International Journal of Materials Science and Applications
2023; 12(6): 83-90
http://www.sciencepublishinggroup.com/j/ijmsa
doi: 10.11648/j.ijmsa.20231206.11
ISSN: 2327-2635 (Print); ISSN: 2327-2643 (Online)

Study the Physical Properties of Zinc-Copper-Iron Alloy Coating the Mild Steel Substrate at Various Iron Content for Automobile Applications

Muhammad Haseeb-U-Rehman, Naseeb Ahmad, Muhammad Abbas, Abbas Ayoub

Institute of Physics, Khwaja Fareed University of Engineering and Information Technology, Rahim Yar Khan, Pakistan

Email address:

haseeb.khanhk1992@gmail.com (Muhammad Haseeb-U-Rehman), naseeb.ahmad@kfueit.edu.pk (Naseeb Ahmad), aeoabbas@gmail.com (Muhammad Abbas), abbasayoub2365@gmail.com (Abbas Ayoub)

To cite this article:

Muhammad Haseeb-U-Rehman, Naseeb Ahmad, Muhammad Abbas, Abbas Ayoub. (2023). Study the Physical Properties of Zinc-Copper-Iron Alloy Coating the Mild Steel Substrate at Various Iron Content for Automobile Applications. *International Journal of Materials Science and Applications*, *12*(6), 83-90. https://doi.org/10.11648/j.ijmsa.20231206.11

Received: September 13, 2023; **Accepted**: October 20, 2023; **Published**: December 14, 2023

Abstract: The Zinc-Copper-Iron alloy was employed as a surface coating material on a mild steel substrate by the electrochemical deposition to investigate the inherent physical characteristics of underlying Zinc-Copper-Iron alloy material. The metallic films were deposited on the substrate with various Iron contents to investigate what sort of effects Iron content has. For this purpose, four samples (Zinc-Copper, Zinc-Copper-xIron) of Zinc, Copper, and Iron alloy coating on a mild steel substrate were prepared. The electrolytic bath employed in the deposition process was composed of a solution containing 0.15M Zinc Sulfate ($ZnSO_4$), 0.15M Copper Sulfate ($CuSO_4$), and varying concentrations (ranging from 0.00M to 0.09M) of Iron Sulfate Heptahydrate ($FeSO_4.7H_2O$), alongside 0.25M boric acid H_3BO_3) serving as a buffer. This study maintained specific operational parameters at predefined values, including a deposition time of 15-20 minutes, a temperature of 50°C, a current density of 20mA cm^{-2}, and a pH level of 3. The investigation centered on the analysis of the crystallographic properties of the ternary alloy coating consisting of Zinc, Copper, and Iron, the examination of surface morphology, and the evaluation of mechanical characteristics. The experimental outcomes stemming from the electro deposition process, employing various concentrations of Iron, revealed several noteworthy observations. Specifically, the surface exhibited increase in smoothness, a reduction in average grain size (from 12.3 to 9.7μm) and a general diminishing trend in both lattice constants (from 3.615 to 3.608Å) and crystal size (from 105.898 to 85.944nm).

Keywords: Electro Deposition, Zn-Cu-Fe Alloy, X-Ray Diffraction, Mild Steel Substrate, Thickness, Morphology

1. Introduction

The invention of Nanoscale technology and its potential led to the splitting increase in the research field of alloys. It is due to its Nanocrystalline building [1]. Extensive substances are developed by vacuum, chemical, spray, and Sol-Gel methods. But these methods need expensive instruments and high-grade procedure control with a lot of loss of substances [1, 2]. Electrochemical deposition or simple electro deposition is a well-appointed technique for the fabrication of films onto the conducting base (substrate) using a current source [3]. Electrochemical deposition parameters control the composition, phase structure, and surface morphology of the materials [3-5]. The working potential has a stout effect on the composition, morphology, and phase structure of alloys [5, 6]. Electrochemical deposition is an advanced technique and is widely used by researchers in various fields. It is due to its variety of applications such as magnetic materials and catalysts [7]. Its benefit is that the content produces films on a large scale in a relatively short time without sacrificing accuracy.

Zinc (Zn) is named a post-transition metal. The molar mass of which is 65.38$gmol^{-1}$. The crystalline configuration of Zinc (Zn) exhibits a Hexagonal Closed Packed (HCP) lattice structure. Zinc and its alloy compositions are renowned for their robust ductility and corrosion-resistant attributes, and are classified as transition metals. Zinc coatings exhibit exceptional characteristics, including high weld ability and paint ability operates [8]. Zinc Oxides find

application within nuclear reactors as a corrosion-inhibiting substance, serving to safeguard rubber-based polymers and plastics against the deleterious effects of ultraviolet radiation. Notwithstanding its indispensable role in immune system function, it is crucial to exercise prudence regarding Zinc consumption, as excessive intake can lead to toxicological repercussions, thus necessitating a careful balancing act to address health-related apprehensions. Furthermore, the inherent brittleness of unalloyed Zinc renders it unsuitable for diverse manufacturing processes. Hence, alloying it with Copper emerges as a pragmatic solution, yielding composite materials aptly suited for the construction of architectural building facades. Copper (Cu) is also a transition metal. The molar mass of Copper is $62.3 gmol^{-1}$. Its crystal structure is Face Centered Cubic (FCC). Due to its strong electrical conductivity, wires and cables made of Copper have been consumed extensively for centuries. A large number of electrical devices depend on copper wiring because of its whole host of inherent beneficial characteristics. These characteristics are creep resistance, low thermal expansion, malleability, and ease of installation. Incomparable characteristics of Copper such as durability, rust resistance, and electromagnetic and lighting shielding make it replaceable in the field of architecture. The biostatic nature of copper is the reason that's why Copper alloys are consumed expansively in the aquaculture industry. Good electro-catalytic activity towards the Oxidation of glucose in the alkaline medium is observed in Copper and its Oxides [9]. Copper shows antibacterial properties and is consumed to create antibacterial composites. Example, examples are Cu-bearing Titanium alloy and Cu-bearing hardened steel [10]. When it comes to health concerns, copper is not hazardous to the $100mg\ m^{-3}$ exposure limit. As mentioned by the IDLH it is immediately dangerous to life and health.

Copper and copper-based alloys have extensive utilization across diverse domains since antiquity, owing to their coveted amalgamation of physical attributes. Copper, by virtue of its intrinsic softness, poses challenges in mach inability. It boasts an extraordinary heat dissipation capacity. Furthermore, Copper exhibits remarkable resistance to corrosion across a spectrum of environments, encompassing atmospheric conditions, marine settings, and select industrial agents. Augmentation of mechanical and corrosion-resistant characteristics in Copper is achievable through alloying. It is clear that a majority of Copper alloys do not readily undergo hardening or reinforcement via conventional heat treatment techniques. Consequently, enhancements in their mechanical properties necessitate the utilization of cold working or solid solution composition [11].

Iron (Fe) is placed before Cobalt in the periodic table, having a molar mass of $55.84 gmol^{-1}$. Being the fourth most abundant component in the world outside, it represents more than 90% of wide-arriving metal manufacture. To satisfy the strict requirements of numerous industrial applications, Iron must possess thermal stability, soft-magnetic characteristics, and electrical permeability. Iron is extremely versatile, as seen by the fact that it is used so frequently due to its remarkable qualities and cost-effectiveness. Due to its ferromagnetic properties, Iron's status as a transition metal further increases its usefulness, notably in applications like magnetic RAM and micro-electromechanical systems. Hardness, ductility, and corrosion resistance all significantly improve when Iron is incorporated into a Zn-Cu alloy, among other properties. As a result, for Iron and Iron-based alloys to efficiently perform their intended duties, they must possess thermal stability, magnetism, and electrical permeability. It is found that ternary Zn-Cu-Fe alloy is eco-friendly and delivers good adhesion. Moreover, this ternary alloy coating reduces bond degradation in a hot and humid atmosphere [12].

Un-doughtily, both Zinc and Copper possess incomparable unique characteristics. Researchers have combined both these metals, forming a Zn-Cu binary alloy. As a result of this benefits are visible in the fields of electronics, architecture, and so on. Enhanced rust and wear resistance make it a potential candidate to form surface coatings. As compared to binary alloys, with time, ternary alloys are more applicable on the commercial scale. A ternary alloy is a combination of three elements, where the emerging material may be differing in character from the constituents. Apart from character, these alloys also cut down on the overall expense. The third element plays an essential role in the character of the ternary alloy. Hence, these days' researchers are working on ternary alloys to utilize the character of three elements into one. They are expecting the resulting alloy to meet the standards to date and be up to the mark.

The main purpose of this research project is to put a Zn-Cu-Fe alloy onto the underlying material in order to improve the mechanical properties of mild steel. Construction, automobile production, mechanical engineering, general purpose fabrication, fencing, structural frameworks, furniture parts with various geometries, pipelines, residential fences, and numerous commercial industries are just a few of the areas where mild steel is widely used. However, mild steel has a number of inherent flaws, most notably a propensity for corrosion and deterioration. Zn-Cu-Fe ternary alloy coatings are used in an effort to address these problems due to the remarkable mechanical and aesthetically pleasing qualities that Iron and Copper impart. These coatings are being used in specialized industries such as in the production of ceramics, die-casting stamping dies, medical equipment, rubber products, and machine bearings.

2. Materials and Methodology

Electro deposition is the method, which is used to deposit films in our study. It has been chosen due to its various advantages over the other commonly used methods. It is a small version of electrolytic deposition, which is a common method to produce a thin film on a metal plate. It works on the electrolysis principle, for example, by using an electric current to remove the cat-ions of a predictable material from the solution and cover the substrate with a film.

Electro deposition is preferred over its rival methods due to

its credibility and lower cost. It is also a suitable method as it does not require any temperature or pressure variation. In addition, this technique has good control over its parameters and retains the ability to coat uneven geometrical surfaces. It is one of the surface plating methods that meet both decorative and functional applications. Apart from this, it upholds appearance, extends life, and enhances material properties. For the production of thin films, high deposition rates and low toxicity are prerequisites. It is due to electro deposition that dense coatings with smooth surfaces are obtained.

To experiment, some different steps are used and then contain our desirable results;

2.1. Substrate Pre-Treatment

Before electro deposition, the substrate of mild steel was physically polished with increasing first-rate grades of emery paper. After that then the substrates were washed with distilled water, then washed with ethanol, dried, and then at the end weighed. All the steps were taken to make the substrate contamination free and to favor the design of smooth thin films. Except for a surface area of $1cm^2$ where the deposition was desired, the whole sheet was covered with Teflon tape. The other side is covered with adhesive tape to avoid excess ions and to uphold excellent deposition.

2.2. Electro Deposition Procedure

A 50mL Pyrex glass beaker that underwent a thorough cleaning process that included rinsing with distilled water and then cleaning with ethanol was used for the experimental procedures. The beaker was then used in each experimental bath after being dried with hot air in a subsequent step. Anode was located inside a graphite cell and had a slightly greater surface area than cathode in a two-electrode cell design. Cathode was made of low carbon steel and had a surface area of $1cm^2$. The anode rod underwent a rigorous polishing procedure that progressed from grade 3 to grade 0 emery paper, with the processes carried out in that order. The anode underwent a series of washing procedures before being exposed to ethanol.

Electrolyte baths are prepared by using the composition of chemicals given in Table 1.

When an electric current is delivered to the anode in the context of electrochemical reactions, metal ions go through an oxidation process that causes them to dissolve in the electrolyte solution nearby. As a result, there is a decrease in the amount of liquid metal ions in the electrolyte solution. The interfacial dynamics at the solution-cathode interface affect the capacity of these dissolved metal ions to undergo electro deposition at the cathode.

Table 1. *Bath compositions for electro deposition of all samples.*

Bath Composition	Concentration (M)				Operating Parameters
	Bath 1	Bath 2	Bath 3	Bath 4	
$CuSO_4$	0.15	0.15	0.15	0.15	pH = 3
$ZnSO_4$	0.15	0.15	0.15	0.15	Temperature = 50°C
$FeSO_4.7H_2O$	0.00	0.03	0.06	0.09	Current density = 20mA cm^{-2}
H_3BO_3	0.25	0.25	0.25	0.25	Saccharin = 0.000218M

2.3. Substrate Post-Treatment

After electro deposition, the substrate was removed. The thin films were dried and the substrates were weighed each time to determine the difference in weights for electro deposition. A difference of 20 to 50mg was observed first in the weights of the substrates. The masses measured before and after the deposition process are shown in the form of Table 2. The films were conserved in an airtight box with electroplating tape for characterization.

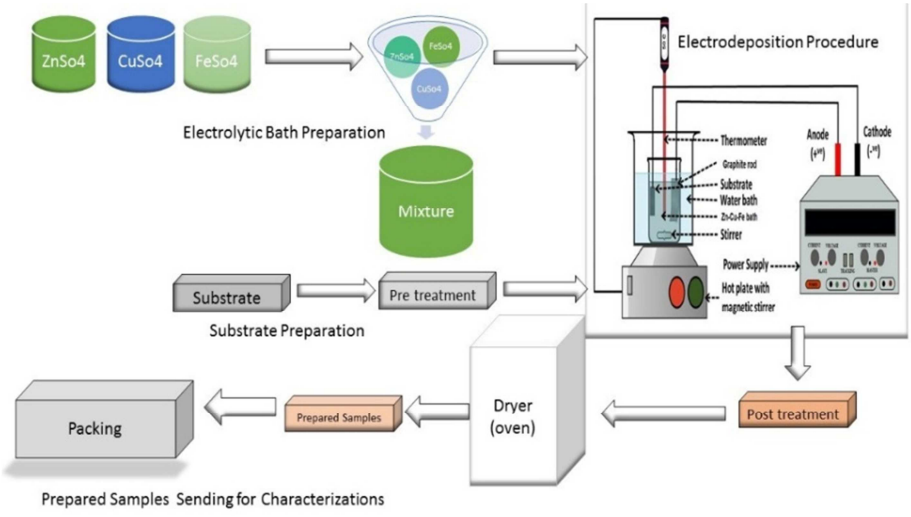

Figure 1. *Schematic diagram of electro deposition procedure [13].*

Table 2. *Mass differences of thin films before and after deposition.*

Sample No.	Thin Films	Deposited Mass (mg)		Mass differences (mg)
		Before	After	
1	Zn-Cu	1480.00	1530.00	50.00
2	Zn-Cu-0.9Fe	1450.00	1490.00	40.00
3	Zn-Cu-1.8Fe	1590.00	1620.00	30.00
4	Zn-Cu-2.7Fe	1520.00	1540.00	20.00

X-ray diffraction (XRD) examination using a Cu-K radiation source was used to explore the crystalline structures of ternary Zn-Cu-Fe alloy coatings. A scanning zone, designated as Scan zone 2, was established with a step size of 0.05° and a scan rate of 0.01°s^{-1}, covering an angular range of 5° to 80°. A Cu-K source running at 45kV accelerating voltage and 40mA emission current was used to acquire XRD patterns. A variety of magnifications, specifically between 40x and 2000x, with varied resolutions ranging from 20-500µm and 1µm, respectively, were used for Scanning Electron Microscopy (SEM) imaging. The SEM device ran at an accelerating voltage of 5kV. A Vickers hardness tester and a mechanical properties measurement instrument were used to determine the mechanical properties of the electrodeposited ternary Zn-Cu-Fe alloys. The test was carried out at room temperature, with a standard load of 200gf applied for 10s to examine the material's mechanical properties.

3. Results and Discussion

3.1. Thickness

The thickness of the coating was calculated using the following mathematical expression [14, 15].

$$t = m/(A\ \rho_{av}) \quad (1)$$

't' is the thickness of the deposited material, where 'm' stands for the mass of the material deposited onto the substrate, 'A' is the area occupied by the deposited material, and ' ρ_{av} ' stands for the average density of the deposited alloy. The data obtained from "(1)" is given in Table 3.

Table 3. *Concentration of Fe, deposited mass, density, and thickness of Zn-Cu-Fe coating alloys.*

Sample No.	Concentration of Fe (mg)	Mass (mg)	Density (mg/mm^3)	Thickness (µm)
1	0.000	50.000	8.032	63.000
2	900.000	40.000	8.025	50.000
3	1800.000	30.000	8.019	37.000
4	2710.000	20.000	9.013	25.000

A graph is drawn between the thickness of an investigated alloys and different Fe concentrations as shown in Figure 1.

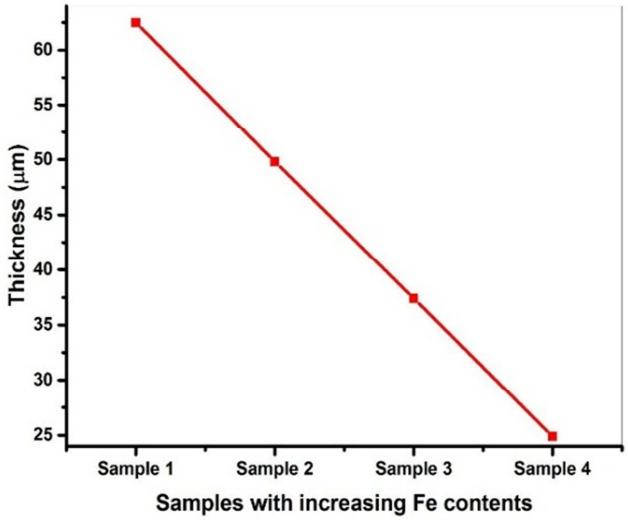

Figure 2. *Thickness of Zn-Cu and Zn-Cu-Fe coating alloys at various concentrations of Fe.*

The thickness fluctuations inside the Zn-Cu and Zn-Cu-Fe coating alloys across different Fe concentrations are shown schematically in Figure 2. A consistent decrease in estimated thickness was seen when samples were deposited at a current density of 20mA cm^{-2}, ranging from 63 to 25µm for samples 1 through 4.

Starting with a thickness of 63µm for sample 1, there was a noticeable decrease in average thickness as the amount of Fe in the electrolyte bath rose to 2710mg. The observed reduction to 25µm was the effect of this. The coating thickness also showed a significant loss, which was notably noticeable between samples 1 and 2, where it dropped by more than 0.2 times. It is possible to blame this drop on the improved surface smoothness and the [16].

3.2. Structure Determination and Phase Analysis

An X-ray diffractometer was used to investigate the phase structure, lattice parameters, and grain size properties of binary Zn-Cu and ternary Zn-Cu-Fe alloys deposited onto mild steel substrates. The relevant X-ray diffraction (XRD) characteristics were calculated using Bragg's and Scherer's equations, which are well-established methods in XRD analysis and are shown in Table 4.

Table 4. *Structure parameters obtained from XRD of Zn-Cu-Fe coatings.*

Sample No	2θ (degrees)	Lattice Constant (Å)	Inter planner spacing's (Å)	Miller indices (hkl)	Crystallite size (nm)	Crystal structure
1	43.60 50.73 74.35	3.605	1.716	111 200 220	65.411	FCC

Sample No	2θ (degrees)	Lattice Constant (Å)	Inter planner spacing's (Å)	Miller indices (hkl)	Crystallite size (nm)	Crystal structure
	43.30			111		
2	50.40	3.615	1.725	200	105.898	FCC
	73.10			220		
	43.60			111		
3	50.70	3.611	1.717	200	101.925	FCC
	74.20			220		
	43.40			111		
4	50.50	3.608	1.723	200	85.944	FCC
	74.03			220		

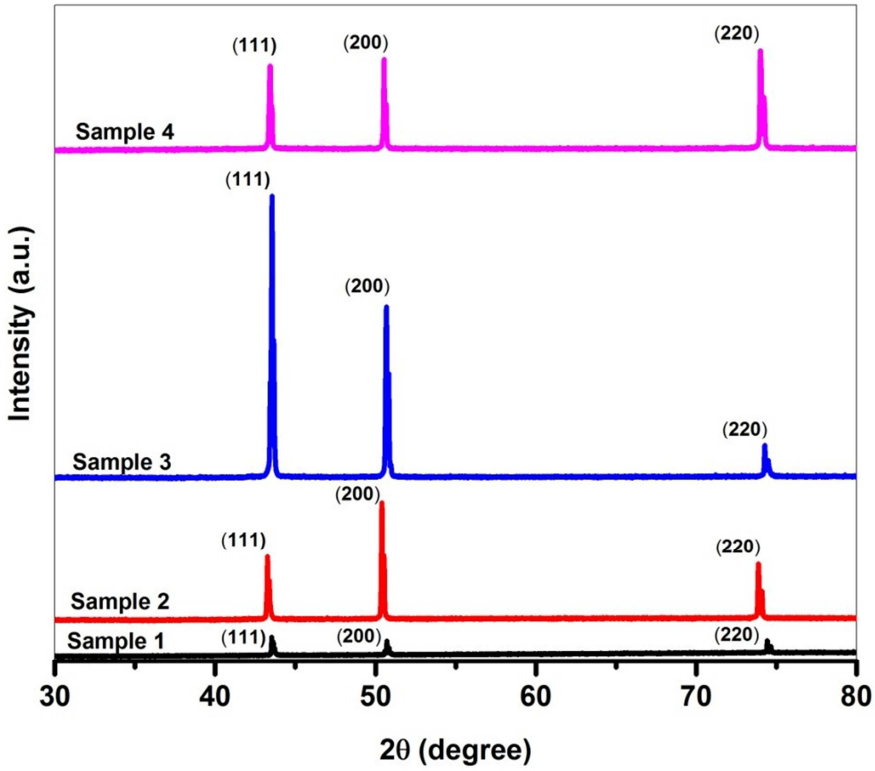

Figure 3. *XRD patterns of Zn-Cu-Fe coating alloys with different concentrations of Fe.*

Figure 3 depicts a graphical representation of the crystal structure of Zn-Cu-Fe alloy thin films placed on a mild steel substrate. The graph depicts intensity as a function of 2θ. Each sample has three different peaks with differing intensities and Miller indices of (111), (200), and (220). The presence of three specific crystallographic planes (111), (200), and (220) proves clearly the FCC (Face-Centered Cubic) crystal structure for the analyzed samples. It is also worth noting that the formation of this FCC crystal structure is perpendicular to the plane of the mild steel substrate. In contrast, whereas Zinc (Zn) has an HCP (Hexagonal Close Packed) crystal structure, copper (Cu) has an FCC structure, and Iron (Fe) have two unique crystal structures at ambient temperature, which are FCC and BCC (Body Centered Cubic). The intriguing observation of peak shifts from left to right may be attributed to a variety of factors, including changes in stoichiometric composition caused by doping, potential instrumental inaccuracies during measurements, and changes in micro structural parameters caused by changes in stress or temperature conditions [17]. The graph also shows an interesting trend: when the peak positions change towards lower angles, the intensity increases over samples 1–3. This remarkable observation is due to the increased density of crystallographic planes caused by the addition of Iron (Fe) in the electrolyte bath [18]. This impact is especially noticeable in the case of FCC (Face Centered Cubic) metals, which have greater deformability than BCC (Body Centered Cubic) and HCP (Hexagonal Close Packed) metals, making them more ductile—a crucial attribute in alloy formation [19].

The FCC crystal structure seen in our investigation matches the predicted result and has an average lattice constant of 3.62Å. The FCC crystal structure we found in our investigation has an average lattice constant of 3.62Å and is consistent with the expected result. It is crucial to keep in mind that the introduction of more Iron may cause this lattice constant to change. In addition, a modest decrease followed by an increase in inter planar spacing can be seen. Defects resulting from the disorderly arrangement of atoms inside the crystal structure are thought to be the cause of this phenomenon [20].

In Figure 4 shows how the lattice constant and crystal size change in relation to the Fe concentration. Together, Table 4 and Figure 4 show a noticeable trend: after the initial addition of Fe to the system, both the crystal size of the samples and the lattice constant show a substantial rise. When compared to Zn and Cu, Fe's atomic radius is noticeably bigger, which is the cause of these phenomena. However, the crystal size shows a subsequent drop as more Fe content is added to the electrolyte bath. This pattern can be linked to the impact of Fe's lattice constant, which is crucial in regulating these variations.

This trend is primarily driven by the fact that the lattice constant of Fe is smaller when compared to the average lattice parameter of Cu and Zn [21]. As the lattice constant undergoes reduction owing to the rapid proliferation of crystalline atoms and the presence of elements with varying atomic radii [22].

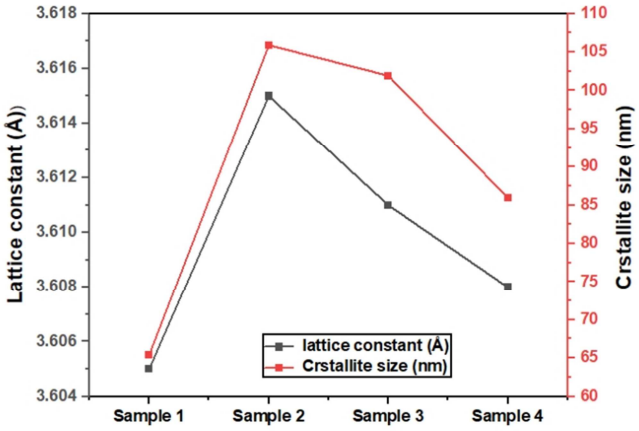

Figure 4. *Lattice constants and crystal sizes at various concentrations of Fe*

3.3. Surface Morphology

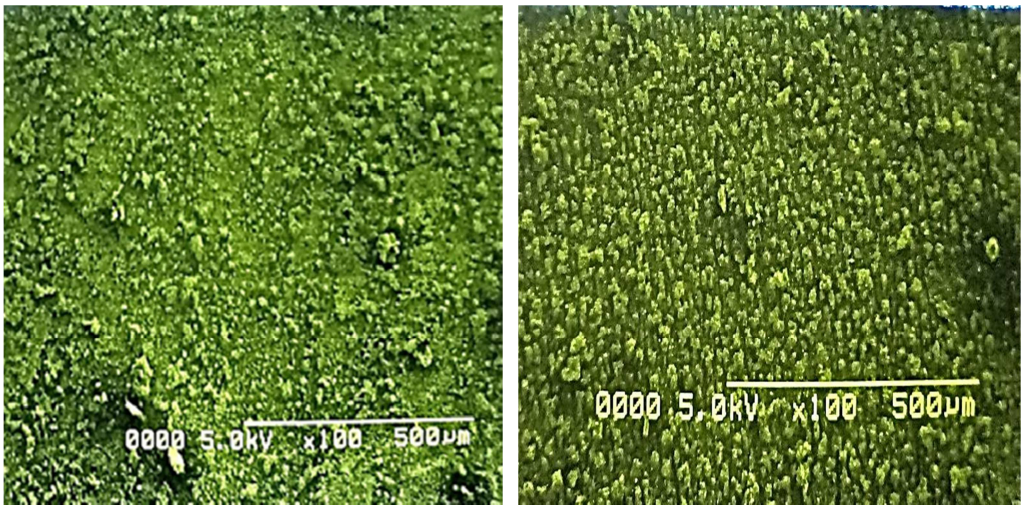

Figure 5. *Surface Morphology of Zn-Cu-Fe alloys without and with Fe content.*

Figure 5 illustrates the surface properties of the alloy coatings; the morphological investigation demonstrates that the Zn-Cu coating alloys have very large average grain sizes of 12.3µm. Two notable changes are noticed with the addition of an increased Fe content in the Zn-Cu-Fe alloy, reaching a concentration of 28%. To begin with, the average grain size decreases to 9.7µm. Second, the grain shape changes from bigger spherical formations to somewhat smaller spherical configurations.

This observed change in grain shape could be attributed to a number of variables, including the potential improvement of mechanical qualities, reduced mass deposition, and the attainment of a more uniform coating over the substrate surface variance.

3.4. Mechanical Properties

We used specialized testing equipment, specifically the Shimadzu AGX-057B and AKASHI HM-102, to determine the mechanical properties of the electrodeposited ternary Zn-Cu-Fe coating alloys.

The results of these mechanical properties micro strain, elastic constant, yield stress, ultimate tensile stress and elongation are shown in Table 5.

Table 5. *Concentration of Fe and mechanical properties of coated alloys.*

Sample	Concentration of Iron (mg)	Ultimate Tensile Strength (MPa)	Micro Hardness (HVN)	Yield Stress (MPa)	Elastic Modulus (GPa)	Elongation (%)
Substrate		336.90	254.82	240.68	200.96	18.35
Zn-Cu Alloy	0.00	340.50	316.54	255.54	221.60	38.99
	900.00	367.70	374.06	257.88	232.56	39.99
Zn-Cu-xFe Alloy	1800.00	389.24	414.58	259.10	239.69	40.77
	2710.00	413.34	434.52	262.65	243.44	41.00

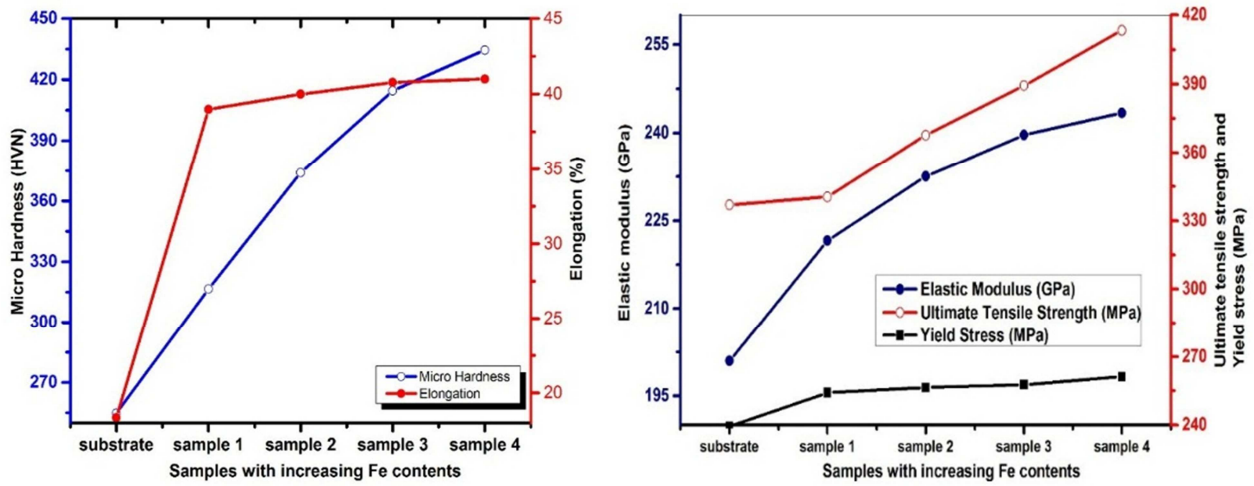

Figure 6. *Micro hardness, Elongation, Elastic modulus, Ultimate tensile strength, and Yield stress at various concentrations of Fe.*

The mechanical characteristics of the extruded alloys are presented in detail in Figure 6(a, b). Clearly, when the Fe concentration rises, the hardness shows a noticeable and gradual improvement. In particular, we notice a progressive change from a hardness value of 316.54HVN for the Zn-Cu alloy to 374.06HVN for the Zn-Cu-0.9Fe alloy, and finally to a remarkable 434.52HVN for the Zn-Cu-2.7Fe alloy. Furthermore, the elongation values show an increased trend, rising from 38.99% for the Zn-Cu alloy to 39.99% for the Zn-Cu-0.9Fe alloy and then to 40.77% for the Zn-Cu-1.8Fe alloy. It is interesting that the Zn-Cu-2.7Fe alloy's elongation exceeds that of the Zn-Cu alloy by a factor of more than two [23].

We observe a minor rise in yield strength (YS) and tensile strength (UTS), but a large increase in elongation, with the increasing augmentation of Fe content. In particular, the UTS values show a progressive increase from 340.5MPa for the Zn-Cu alloy to 367.7MPa for the Zn-Cu-0.9Fe alloy and finally to 413.34MPa for the Zn-Cu-2.7Fe alloy. The elastic modulus's behavior shows a similar pattern [24].

These findings' combined mechanical properties highlight the advantageous effects of increasing the Fe concentration. This enhancement has a positive impact on many mechanical properties of the samples, including their hardness, ultimate tensile strength, yield stress, elastic modulus, and elongation. This enhancement is related to the fact that Fe is intrinsically harder than Zn and Cu [25].

4. Conclusion

To conclude the present study of the ternary Zn-Cu-Fe alloy, we can say that it is electrodeposited on a mild steel substrate at room temperature pH and its current density was kept constant during the electro deposition. Some characteristics like XRD parameters, the grain size of SEM imagining, and mechanical properties like hardness, UTS, Yield stress, thickness, modulus of elasticity, and elongation were investigated. The film of Zn-Cu-Fe alloy on mild steel substrate becomes smoother with the addition of Fe content. XRD parameters like inter planner spacing, miller indices, crystalline size, and crystal structure were investigated using Bragg's and Scherer's equations. Results showed that the decrease in average grain size of the Zn-Cu-Fe alloy was caused by increased Fe content and the value of the ionic radii after deposition decreased.

From the results, it is revealed that mechanical properties like hardness, UTS, Yield stress, modulus of elasticity, and elongation of samples are increased due to the increment in the concentration of Fe and the average grain size of the samples decreased because it becomes harder to stand for natural elements and to utilize the complexity and in cashing applications.

Acknowledgments

It is difficult to overstate my gratitude to my supervisor, Dr. Naseeb Ahmad (Assistant Professor Department of physics). His sage advice, insightful criticism, sympathetic attitude, enthusiastic supervision especially during experimental work, and patient encouragement aided the writing of this manuscript.

References

[1] Baskaran, I., T. S. Narayanan, and A. Stephen, Pulsed electrodeposition of nanocrystalline Cu–Ni alloy films and evaluation of their characteristic properties. Materials Letters, 2006. 60(16): p. 1990-1995.

[2] Cazottes, S., et al., Correlation between microstructure at fine scale and magnetic properties of magnetoresistive Cu80Fe10Ni10 ribbons: Modeling of magnetization. Journal of magnetism and magnetic materials, 2013. 333: p. 22-29.

[3] Seet, H., et al., Development of Ni80Fe20/Cu nanocrystalline composite wires by pulse-reverse electrodeposition. Journal of alloys and compounds, 2008. 449(1-2): p. 279-283.

[4] Silva, B., et al., Microwave absorption of electroplated NiFeCu/Cu multilayers deposited directly on Si (100) substrates. Journal of Magnetism and Magnetic Materials, 2016. 420: p. 23-27.

[5] Esmaili, S., M. Bahrololoom, and L. Peter, Magnetoresistance of electrodeposited NiFeCu alloys. Thin Solid Films, 2012. 520(6): p. 2190-2194.

[6] Goranova, D., G. Avdeev, and R. Rashkov, Electrodeposition and characterization of Ni–Cu alloys. Surface and Coatings Technology, 2014. 240: p. 204-210.

[7] Zin, V., K. Brunelli, and M. Dabalà, Characterization of Cu–Ni alloy electrodeposition and synthesis of nanoparticles by pulsed sonoelectrochemistry. Materials Chemistry and Physics, 2014. 144(3): p. 272-279.

[8] Rashwan, S., Study on the behaviour of Zn Co Cu alloy electroplating. Materials chemistry and physics, 2005. 89(2-3): p. 192-204.

[9] Yang, F., et al., Pd–Cu alloy with hierarchical network structure as enhanced electrocatalysts for formic acid oxidation. International Journal of Hydrogen Energy, 2016. 41(16): p. 6773-6780.

[10] Suneesh, P., et al., Co–Cu alloy nanoparticles decorated TiO2 nanotube arrays for highly sensitive and selective nonenzymatic sensing of glucose. Sensors and Actuators B: Chemical, 2015. 215: p. 337-344.

[11] Pellicer, E., et al., A comparison between fine-grained and nanocrystalline electrodeposited Cu–Ni films. Insights on mechanical and corrosion performance. Surface and Coatings Technology, 2011. 205(23-24): p. 5285-5293.

[12] Buytaert, G. and Y. Luo, Study of Cu–Zn–Co ternary alloy-coated steel cord in cobalt-free skim compound. Journal of Adhesion Science and Technology, 2014. 28(16): p. 1545-1555.

[13] Fayyaz, O., et al., Enhancement of mechanical and corrosion resistance properties of electrodeposited Ni–P–TiC composite coatings. Scientific reports, 2021. 11(1): p. 5327.

[14] Jeansonne, N., et al., Continuous-flow monitoring of hexuronic acid by carbazole reaction during gel filtration of proteoglycans in urea solutions. Journal of Chromatography A, 1986. 354: p. 524-529.

[15] Imran, M., et al., Investigation of annealing effects on physical properties of chemically prepared copper oxide thin films. Results in Optics, 2023. 10: p. 100331.

[16] Thanu, V. C., C. Andrew, and M. Jayakumar, Electrodeposition of nickel super alloy from deep eutectic solvent. Surfaces and Interfaces, 2020. 19: p. 100539.

[17] Lin, Y.-J., et al., Defects, stress and abnormal shift of the (0 0 2) diffraction peak for Li-doped ZnO films. Applied Surface Science, 2010. 256(24): p. 7623-7627.

[18] Mangenot, S., et al., X-ray diffraction characterization of the dense phases formed by nucleosome core particles. Biophysical journal, 2003. 84(4): p. 2570-2584.

[19] Osetsky, Y. N. and D. J. Bacon, Comparison of void strengthening in fcc and bcc metals: large-scale atomic-level modelling. Materials Science and Engineering: A, 2005. 400: p. 374-377.

[20] Guc, M., et al., Conductivity mechanisms and influence of the Cu/Zn disorder on electronic properties of the powder Cu2ZnSn (S1-xSex) 4 solid solutions. journal of materials research and technology, 2021. 13: p. 2251-2259.

[21] Delhez, R., T. H. Keijser, and E. Mittemeijer, Determination of crystallite size and lattice distortions through X-ray diffraction line profile analysis. Fresenius' Journal of Analytical Chemistry, 1982. 312(1): p. 1-16.

[22] Kumar, D., M. Singh, and A. K. Singh. Crystallite size effect on lattice strain and crystal structure of Ba1/4Sr3/4MnO3 layered perovskite manganite. in AIP Conference Proceedings. 2018. AIP Publishing.

[23] Ranjbar-Mohammadi, M., et al., Electrospinning of PLGA/gum tragacanth nanofibers containing tetracycline hydrochloride for periodontal regeneration. Materials Science and Engineering: C, 2016. 58: p. 521-531.

[24] Yue, R., et al., Microstructure, mechanical properties and in vitro degradation behavior of novel Zn-Cu-Fe alloys. Materials Characterization, 2017. 134: p. 114-122.

[25] Thilipkumar, K., R. Sellamuthu, and R. Saravanan, An investigation on the microstructure, wear rate and hardness of Surface alloying Ni-Hard 4 cast iron with Tungsten Using GTA. Materials Today: Proceedings, 2020. 24: p. 548-556.